Practical Vessel Imaging by Computed Tomography in Live Transgenic Mouse Models for Human Tumors

Gordon L. Kindlmann[1], *David M. Weinstein*[1], *Greg M. Jones*[1], *Christopher R. Johnson*[1] *Mario R. Capecchi*[1], *and Charles Keller*[2]

[1]University of Utah and [2]The University of Texas Health Science Center

Abstract

Contrast-enhanced small-animal computed tomography is an economical and highly quantitative tool for serially examining tumor development in situ, for analyzing the network of blood vessels that nourish them, and for following the response of tumors to preclinical therapeutic intervention(s). We present practical considerations for visualizing the vascular network of transgenic mouse tumors. Using a long-acting iodinated triglyceride blood-pool contrast agent, we present optimized scanner acquisition parameters and volume-rendering techniques for examining the intermediate and large vessels of complex spontaneous tumors (e.g., alveolar rhabdomyosarcomas) in transgenic mice. Our findings indicate that multiple-frame, 360–720 view acquisitions were mandatory for clarifying bone and soft tissue from vessel contrast. This finding was consistent in visualizations using a one-dimensional transfer function where voxel color and opacity was assigned in proportion to CT value and a two-dimensional transfer function where voxel color and opacity was assigned in proportion to CT value and gradient magnitude. This study lays a groundwork for the qualitative and quantitative assessment of anti-angiogenesis preclinical studies using transgenic mice. *Mol Imaging* (2005) **4,** 417–424.

Keywords: Computed tomography, small-animal imaging, intravenous contrast, iodinated triglycerides.

Introduction

Transgenic mouse models of human cancer have the potential to be more reflective of human cancers than xenograft models because transgenic mice form tumors in situ, (i.e., in an environment more similar to the human tumor and in the setting of a normal immune system). Small-animal X-ray computed tomography (microCT) is an economical and highly quantitative three-dimensional method for visualizing blood vessels and angiogenesis preclinically [2,9] even in comparison to small-animal magnetic resonance imaging [6]. The goal of this study was to develop practical guidelines for rapid, accurate visualization of intermediate to large caliber (>93 μm) blood vessels for serial assessment of vascularity during preclinical therapeutic trials in living mice. The limitations caused by long scan times for most small-animal CT studies were overcome by using a long-acting blood-pool contrast agent [12]. In this study, we assessed vessels by qualitative visual renderings, although the same optimized acquisition settings would be necessary for quantitative analysis of tumor blood volume, vessel density, vessel caliber, degree of branching, and tortuosity using segmentation analysis.

Materials and Methods

Computed Tomography Scanning

All animals used for this study were treated in accordance with an IACUC approved protocol. Live mice were injected with 0.4 mL/25 g of a 50-mg iodine/mL 150-nm particle diameter iodinated triglyceride blood-pool contrast agent [12] (Fenestra VC; Alerion Biomedical, San Diego, CA) into the distal tail vein using a 25- or 27-gauge needle. Both wild-type C57BL/6 mice and transgenic mice harboring a conditional knock-in of the *Pax3:Fkhr* oncogene, causing alveolar rhabdomyosarcomas, were utilized [5]. Mice were anesthetized with an intraperitoneal injection of 0.3–1 mL/25 g of 2.5% Avertin depending upon whether survival or sacrifice was intended. For minimization of movement artifacts, mice were placed in a custom-built, commercially available isolator (CH Technologies, Westwood, NJ) with continuous airflow delivered by a generic fish tank pump. Volumetric CT of anesthetized mice was performed at 93 μm^3 voxel resolution using an eXplore Locus Small Animal MicroCT Scanner (GE Healthcare, London, Ontario). This volumetric scanner employs a 3500 × 1750 CCD detector for Feldkamp cone-beam reconstruction and is similar in design to other commercially available in vivo scanners under US$300,000 that are commonly operated as regional core facilities

Corresponding author: Charles Keller, Children's Cancer Research Institute, The University of Texas Health Science Center, 8403 Floyd Curl Drive, San Antonio, TX 78229-3900; e-mail: kellerc2@uthscsa.edu.

Received 13 May 2005; Received in revised form 25 May 2005; Accepted 21 June 2005.

(http://ccri.uthscsa.edu). In this study, the platform-independent parameters of current, voltage, and exposure time were kept constant at 430 μA, 80 kV, and 100 msec, respectively. The number of views varied between 180 and 720 and was evenly spaced. The number of frames per view was varied from 1 to 8. Images were reconstructed with the manufacturer's proprietary EVSBeam software, and preliminary visualizations (not shown) were generated with the open-source MicroView program (http://microview.sf.net).

Image Rendering

The tomography volume files computed by the EVS-Beam software were processed with the open-source utilities in Teem (http://teem.sf.net) to generate the slice images, histograms, and volume renderings in the following figures. Other than cropping to the region of interest (head and torso), no other filtering or smoothing was applied to the data. The volume renderings were computed with a standard brute-force ray-casting algorithm, using the framework presented by Levoy [8], which proceeds as follows: for each pixel in the rendering, a geometric ray is cast through the CT volume according to the virtual camera position, and the CT values and gradient vectors are densely sampled along the rays. The gradient vectors are the basis of the synthetic shading which conveys local surface orientation. The value and gradient measurements are performed by convolving the discrete CT volume samples with separable continuous kernels, as described by Möller et al. [10]. For this study we used the Catmull-Rom kernel for value measurement, and the derivative of the uniform cubic B-spline for derivative measurement. Other than early ray termination after hitting a nearly completely opaque region, no optimizations or approximations are employed, resulting in a highly accurate, though computationally intensive, rendering. The computation for each horizontal row of pixels was distributed across 64 CPUs of an SGI Onyx 3800 in a first-come-first-serve manner, resulting in a total rendering time of approximately 1 min. The beta-test of a bundled, graphic user interface (GUI)-based software package encompassing all the abovementioned algorithms was used to generate preview renderings.

Colors and opacities are assigned to the ray sample according to the transfer function, which is parameterized by either CT value (in the case of 1-D transfer functions), or both CT value and gradient magnitude (in the case of 2-D transfer functions). Transfer functions were manually adjusted based on guidance provided by CT value histograms (Figure 1). For this study, the strategy of 1-D transfer function adjustment was to assign maximal opacity to the broadest range of high CT values (belonging to bone), without impinging on the range of CT values associated with soft tissue. Reducing tomography artifacts significantly facilitates this particular task, by narrowing the value ranges associated with each material (Figure 2). For 2-D transfer functions, the transfer functions were created with guidance from a joint histogram of CT value and gradient magnitude, based on the considerations outlined by Kindlmann and Durkin [7]. Anatomical landmarks were verified with an atlas of surface and cross-sectional mouse anatomy [3].

Results

Vessel Identification is Critically Dependent upon Accurate Soft Tissue Identification and Differentiation from Bone

Tumors in transgenic mice are inherently different from xenografts because the transgenic mouse tumors are often intermingled with bony structures instead of lying in the soft tissue flank. Therefore, vessel imaging in transgenic mouse tumors represents a new paradigm. To determine the best scanner acquisition settings for accurate rendering and visualization of blood vessels from the microCT dataset, we first performed serial scans with different settings on a wild-type C57BL/6 control mouse that had undergone a tail vein injection of 0.4 mL iodinated triglyceride contrast agent (50 mg iodine/mL) 5 min before euthanasia. We used evenly spaced views about a full gantry rotation because prior experience with partially circumferential imaging led to unacceptable artifacts (data not shown). Our instrument is capable of resolutions between 27 and 93 μm isotropic voxel resolution; however, because the higher resolution would decrease the field of view and would increase the radiation dose to the animal above 200 Roentgens (R), we chose to use 93 μm resolution ($<55R$) for this initial study. We anticipated that the use of larger voxels would also lead to minor overestimation of vessel diameters as a result of partial volume effects (e.g., a single voxel partially residing in vessel would be classified as wholly vessel).

With views every 2 degrees of rotation (180 views total), a cogwheel-appearing aliasing artifact of reconstruction was apparent because of too few views (Figure 1A). However, by increasing the number of views to 360 or 720, this artifact dissipated, and by increasing the number of frames averaged per view from 1 to 8, the boundaries of vessels in the neck became increasingly

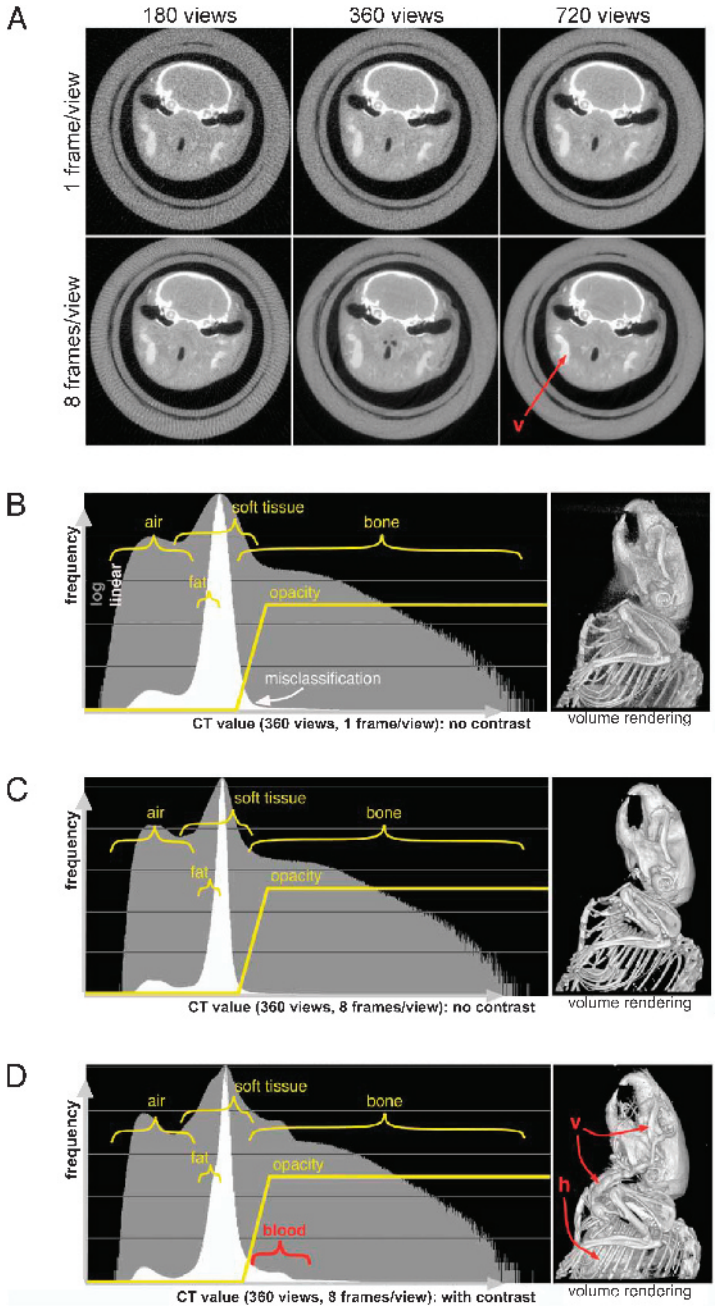

Figure 1. *Scan parameters influence the differentiation between soft tissue, bone, and vascular contrast. (A) In axial head and neck views of live mice administered iodinated triglyceride contrast agent, increased views per scan reduce cogwheel-like aliasing artifacts, whereas increased frames per view improve signal to noise (thereby reducing "speckle"). v = iodinated triglyceride contrast in vessels. (B,C) For live mice without contrast agent, increased frames per view significantly improve the ability to differentiate bone and soft tissue contrast. Histograms (B and C, left) show the distribution of CT (density) values, presented with frequency in linear (white) and logarithmic (gray) scale. A rendering of bone, whereby increased opacity is assigned to voxels with high CT values, is shown to the right of each histogram in (B) and (C). At 1 frame per view, the soft tissue peak is wide and therefore a subset of soft tissue voxels are misclassified as bone in both the histogram (B, left) and the rendering (B, right). At 8 frames per view (C), the soft tissue peak becomes narrower, allowing better distinction between soft tissue and bone. As a result, misclassification is greatly reduced, so that although opacity is assigned to bone, no opacity is assigned to soft tissue thereby clarifying the volume rendering. Note that the bone CT values are a "tail," rather than a peak. (D) In a separate animal injected with the iodinated triglyceride contrast agent, the contrast peak (labeled "blood") is intermediate to soft tissue and bone, but an appropriate threshold can be chosen to distinguish soft tissue from vascular contrast agent and bone. h, heart.*

distinct qualitatively (as signal-to-noise improved). Because the blood contrast agent density was intermediate between bone and soft tissue, we examined the separation of density values (CT values) between soft tissue and bone in a control animal not injected with contrast. We observed the unexpected phenomena that although soft tissue CT values fall into a distinct peak, bone CT value falls into an indistinct "tail." This can be seen by

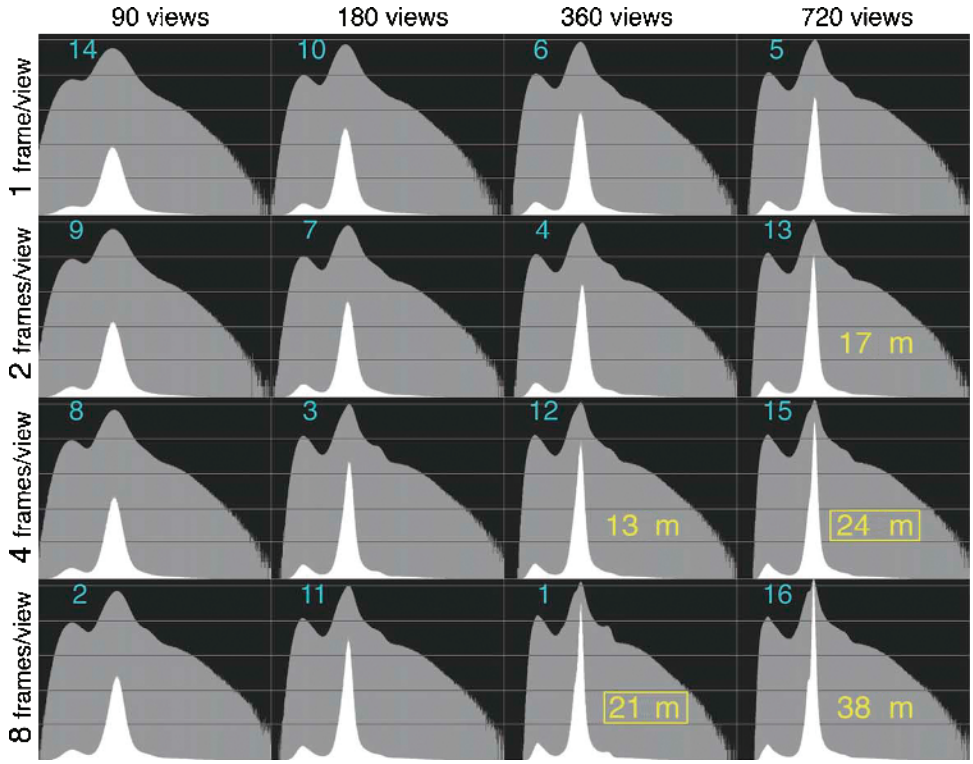

Figure 2. *Optimal scan quality for rendering requires high views/frame and frames/view. A sedated live mouse was administered a single 0.4-mL dose of iodinated contrast agent and after 5 min was given a lethal dose of sedation. The mouse was then serially scanned at different settings for views/scan and frames/view. The objective was to identify a protocol with the narrowest soft tissue peak for the shortest scan time (yellow text; m = minutes). The order of scans is shown in blue text. Acceptable narrowing of soft tissue peaks was found for CT value histograms of scans with 360 or 720 views/scan and 4–8 frames/view. The optimal scan settings were 360 views/scan with 8 frames/view (21 min), and 720 views/scan with 4 frames/view (24 min).*

inspection of the histogram of CT values in Figure 1B. The main peak in the histogram, signifying the most common material, is that of non-contrast-enhanced soft tissue. Bone does not constitute a discernible histogram peak because of both the relatively insignificant number of voxels with bone (due to the thinness of bone), and the widely varying opacities attributable to bone (due to varying bone thickness and density, combined with partial volume effects). Based on these considerations, a high-quality scan is one in which the width of the peak attributed to soft tissue is minimized. This in turn minimizes misclassification of soft tissue voxels and contrast-containing blood vessel voxels during application of volume-rendering transfer functions. The improved distinction between soft tissue and bone with increasing frames per view was demonstrated by choosing the best volume-rendering threshold between the ''peak'' of soft tissue CT values and the ''tail'' of bone CT values using the 1 frame per view scan versus the 8 frames per view scan (Figure 1B and C, respectively). At the higher number of frames per view, with a different animal injected with intravenous contrast, a clear distinction between soft tissue and vessel-contrast-plus-bone could be made (Figure 1D). Note that the CT values of the blood contrast agent are found in a distinct peak when 8 frames/view are used, but it would not have been distinguishable from the wider soft tissue peak of the 1 frame/view scan.

Improving the Signal-to-Noise Ratio of Soft Tissue Requires Longer Scan Times with Increased Numbers of Views and Number of Frames per View

We had hoped that a quality scan for a large field of view could be achieved in less than 20 min so that the duration of anesthesia could be minimized and the throughput of animals maximized. Our goal in performing a test set of scans varying in the number of views and the number of frames/view in a euthanized animal (Figure 2) was to find settings that required the least amount of time but resulted in the narrowest peak of soft tissue CT values. The settings that were most optimal for distinguishing soft tissue, vessel contrast, and bone in subsequent transfer functions for rendering were the 21 min 360 view, 8 frame/view settings and the 24 min 720 view, 4 frame/view settings. The 13 min 360 view, 4 frame/view settings was nearly, but not completely acceptable for subsequent renderings (data not

shown). Although not an intended element of this study, we observed (Figure 2) that the histogram peak attributable to contrast-enhanced vessels seems to increase in width (with a corresponding decrease in height) in the animal following death, suggesting a postmortem diffusion process. This phenomenon would not be expected to occur in live animals, although in live mice the iodinated triglyceride is known to slowly be taken up by the liver over a period of hours [12].

A 2-D Transfer Function Improves the Distinction between Vessel Contrast and Bone during Rendering

Figure 3 compares two types of rendering algorithms available as open source software. The first rendering method, a 1-D transfer function, assigns red color and intermediate opacity to voxels with CT values intermediate between soft tissue and bone (Figure 3A, left). Note that the resultant rendering (Figure 3B, left) appears to have an undesirable red haze overlying the bone cortex. However, using a 2-D transfer function that assigns red color and intermediate opacity to voxels based upon both the CT value and gradient magnitude (Figure 3A, right), the resulting rendering distinguishes bone and vessel contrast more accurately (Figure 3B, right).

Given the significantly improved ability to differentiate vessel contrast from bone using a 2-D transfer function instead of a 1-D transfer function, we examined whether less robust scanning parameters could be used with a 2-D transfer function and still accurately distinguish iodinated triglyceride contrast from bone (Figure 3C). We found that the optimal, 21–24 min scan parameters were still required to prevent misclassification of vessel contrast as bone in control mice.

Even with a 2-D Transfer Function, Optimal Scan Acquisition Parameters are Necessary

Using optimized scan parameters (360 views, 8 frame/view), vascular imaging of a large *Pax3:Fkhr* expressing rhabdomyosarcoma of the lower extremity could be effectively performed on a living mouse that survived the scan, demonstrating arterial and venous vessels with complex branching patterns (Figure 4A). At this resolution, capillary networks could be visualized collectively but individual capillaries could not be distinguished. For comparison, we performed a 720-view, 4 frame/view scan of a different transgenic tumor-bearing mouse that survived the scan (Figure 4B) demonstrating a neck tumor arising from the left sternocleidomastoid. The hypoxic nature of this collagen-rich tumor is evident from its avascularity, yet it aggressively displaces the adjacent normal vessels. We also note that at this resolution (93 μm^3) the thin-walled, large lumen venous vessels are more easily visualized than corresponding the thicker-walled, smaller lumen arterial vessels that run adjacent to them (Figure 4C). Another limitation is that thin-cortex bones, such as the scapula (Figure 4C), were still misclassified as contrast agent. Overall, however, renderings of transgenic mouse tumors are generally very informative when optimized scan settings are used in combination with a 2-D transfer function. As a practical note, the 0.4-mL dose of iodinated triglyceride intravenous contrast is generally well tolerated by mice, but similar results can be achieved with the same scanner parameter settings and a lower 0.2–0.3 mL dose of the contrast agent.

Discussion

The primary goal of this microCT study was to determine optimal techniques for generating quality datasets for analysis of tumor vascular networks in live mice that would be serially scanned. Establishing the minimum necessary, platform-independent scanner parameter settings was accomplished through a combination of histogram analysis and qualitative evaluation of volume renderings. A secondary goal of this study was to demonstrate, through volume rendering, the quality and resolution of the anatomical imaging possible with a long-acting blood pool contrast agent. For both goals, multiple-frame, 360–720 view acquisitions were mandatory for clarifying bone and soft tissue from vessel contrast. This study is a necessary prelude to subsequent quantitative image analysis where signal-to-noise and boundary delineation are critical (e.g., modeling of vasculature network using image segmentation).

Improvements in CT technology are likely to make vessel imaging in transgenic mouse models easier, faster, and more accurate over time. Already, commercially available (but substantially more expensive) scanners exist which can scan an entire mouse at 150 μm isotropic voxel resolution in under 2 sec [6]. This rapid acquisition is useful not only for studying tumor vessel anatomy, but enables study of tumor perfusion and vascular permeability as well. When this acquisition speed can be achieved for higher spatial resolution (15 μm), the ability to study vasculoneogenesis of small arterioles in tumors will be significantly improved. Faster acquisitions will also enable the use of short-lived (clinical), high-iodine content contrast agents instead of low-iodine content blood pool contrast agents, although our experience suggests that contrast agents of intermediate

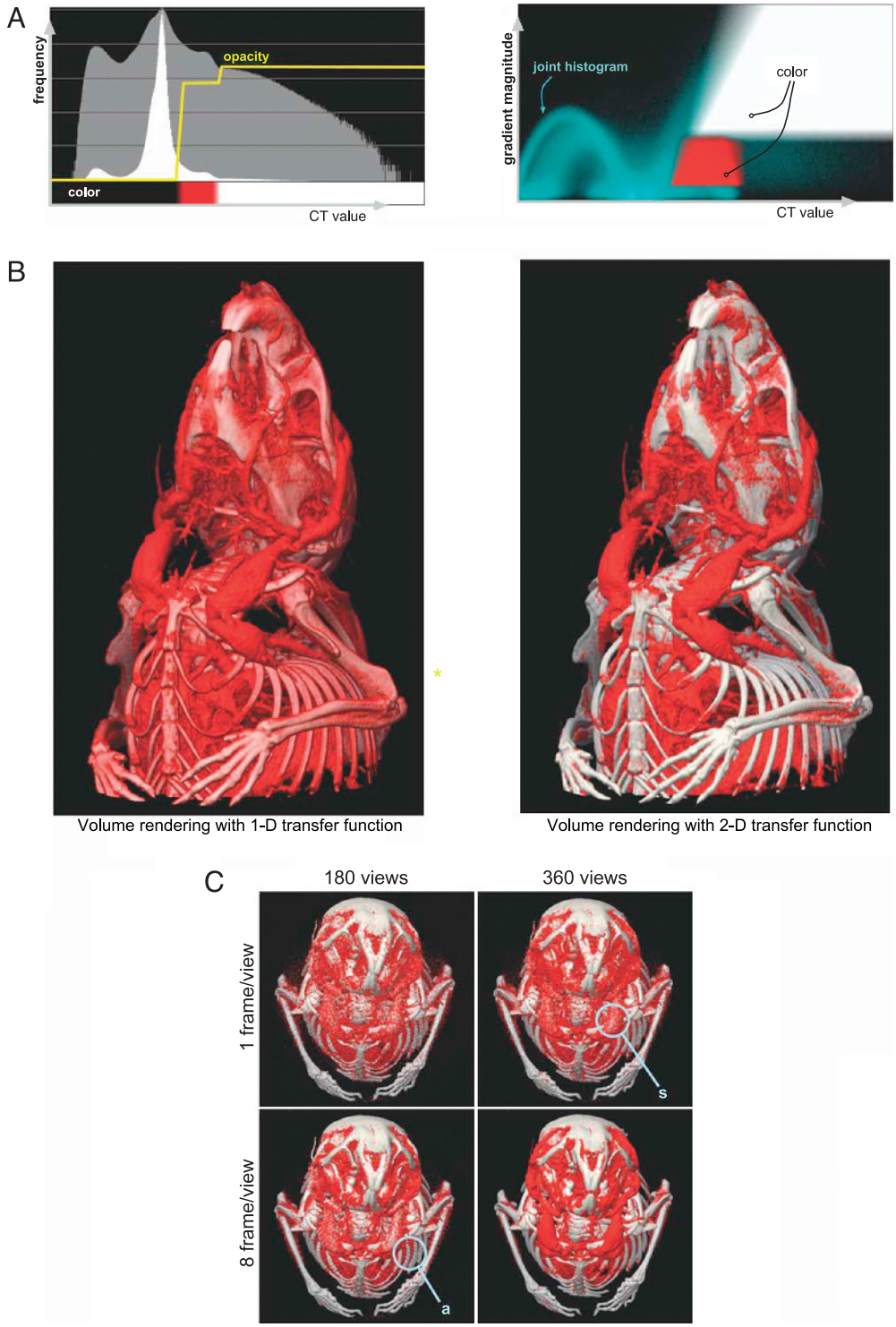

Figure 3. *Complex transfer functions improve rendering of vessel contrast. (A, left panel) For the 1-D transfer function, the CT value histogram is used to guide the assignment of red color and intermediate opacity to the window of CT values associated with the iodinated contrast agent. (A, right panel) For the 2-D transfer function, the plot of CT value and gradient magnitude is used to guide the assignment of color and opacity to those regions of the transfer function domain that are associated with vascular and bone boundaries. Ray-cast volume rendering with 1-D transfer function (B, left panel) and 2-D transfer function (B, right panel). Depth cueing slightly darkens features further from the image plane, helping depiction of three-dimensional structure. The 1-D transfer function misclassifies as blood the intermediate CT values at the outer surface of the bone, giving a superficial red hue to all bones. This effect can be reduced by reducing the opacity associated with red, at the cost of decreasing the visibility of the vessels. The 2-D transfer function largely avoids this problem, by assigning red color only to the lower gradient magnitudes associated with the vessel boundary. (C) Although 2-D transfer functions reduce misclassification vessel and bone at 360 views/scans with 8 frames/view, reducing either views/scan or frames/view to decrease scan time results in similar problems. For example, speckle noise ("s") present in the external jugular vein creates higher gradient magnitudes, as found at the bone surface, resulting in the white regions within the vessel. Cogwheel-like aliasing artifacts ("a") caused by insufficient views/scan are rendered as regular ridges on anatomical surfaces. Therefore, with our instrument we still required a minimum of 21–24 min to produce quality scans suitable for rendering vessels and bone properly.*

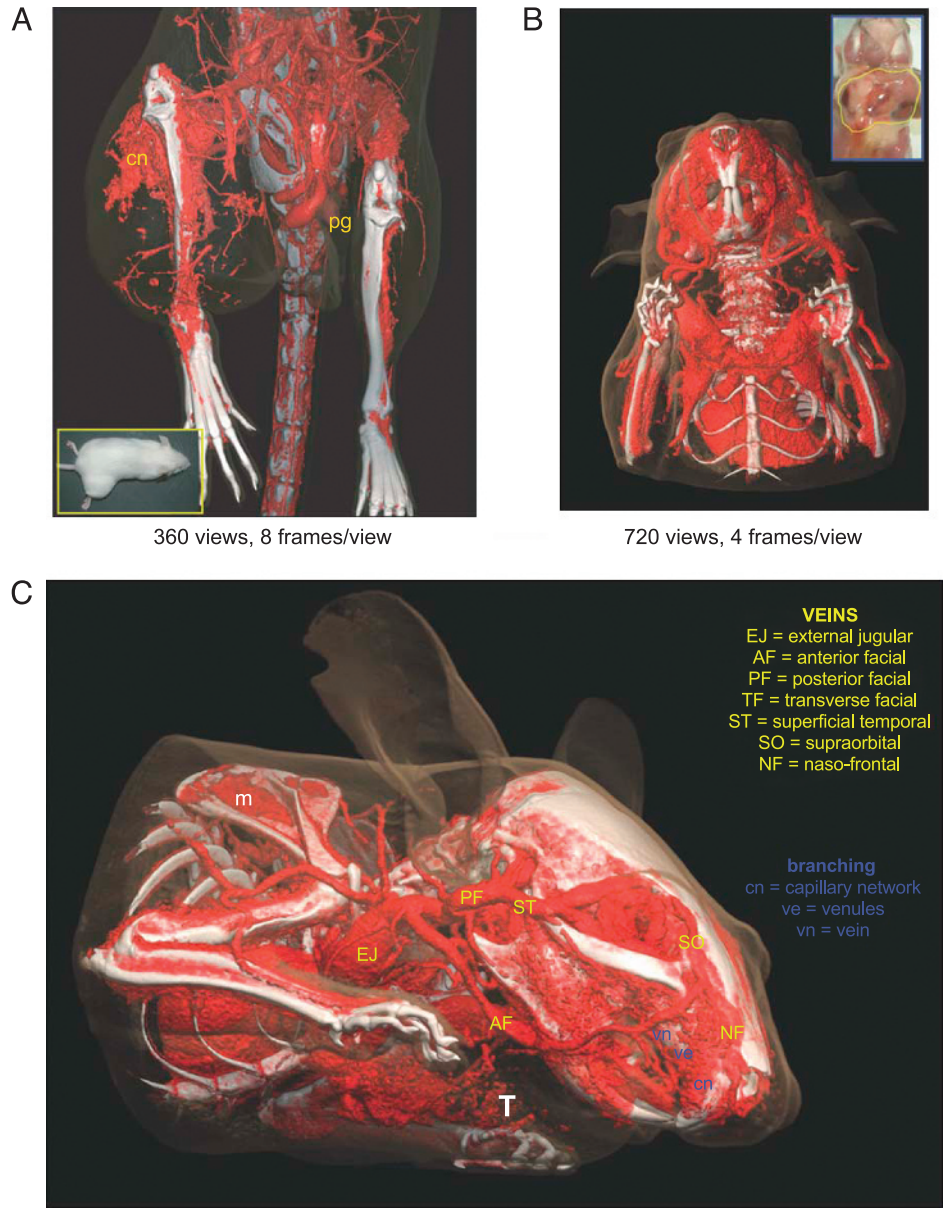

Figure 4. *Optimal scan parameters and 2-D transfer functions are required to visualize vascular networks for tumors in transgenic mice. (A) Example of a right lower extremity tumor (inset) scanned after tail vein injection of 0.4 mL contrast agent in a live mouse at 360 views and 8 frames per view. cn = capillary network; Pg = vasculature-rich preputial gland. (B) Example of a neck tumor (inset, tumor outlined in yellow) scanned after tail vein injection of 0.4 mL contrast agent in a live mouse at 720 views and 4 frames per view. (C) A different point of view of the animal in (B) with vessels labeled. T = tumor; m = misclassified region of scapular bone, rendered as blood.*

density between soft tissue and bone may be most advantageous in the identification of contrast-enhanced vessels. On this note, a continuous (25 min) intravenous infusion of a smaller volume (< 0.2 mL) of clinical contrast agent would be likely be as effective with current microCT scanners as the blood-pool contrast agent used in this study.

By the high-resolution nature of small-animal imaging, mouse models of human tumors are expected to lead and guide clinical studies of tumor vascular biology and anti-angiogenesis therapies which target capillaries. Although xenograft models have been very informative for studying basic mechanism of angiogenesis, orthotopic or spontaneous/in situ (transgenic) mouse models will more accurately reflect host organ effects and are expected to more accurately predict response of human tumors [1]. In 2001, Jain [4] very rightly pointed out the need for better noninvasive imaging in anti-angiogenesis clinical trials, whereby response measures such as vessel diameter, vessel tortuosity, vessel density, vascular permeability, partial pressure of oxygen, and interstitial pressure could be measured. Direct visualization of

capillaries is not yet possible with current instruments because the resolution required would exceed both a safe radiation dose and a safe anesthesia duration for a living mouse. To analyze angiogenesis with current technology, one would rely on surrogate markers such as total tumor contrast-enhanced blood volume, or change in the structure of amalgamated capillary networks as they appear in scans at 46–93 μm resolution (Figure 4A). With anticipated advances in instrumentation, X-ray CT holds the best potential to define anatomical measures of vessel diameter, tortuosity, and density for tumors whose capillary diameters can range from 11 to 15 μm [11]. Other modalities such as magnetic resonance may be equally or better suited to defining tumor boundaries, permeability, oxygenation, and interstitial pressure. Therefore, co-registration of serial multimodality images of the same tumor may become the standard for preclinical and clinical anti-angiogenesis studies. A great deal of work remains to be done for instrumentation development, scan optimization, and postprocessing analysis, but the field is off to an encouraging start.

Acknowledgments

This work was supported in part by a K08 award to C. K. from the National Cancer Institute (1K08 CA90438-01) and an NIH NCRR Center award to C. R. J. (P41RR12553). We thank Alerion Biomedical for samples of their iodinated triglyceride contrast agents. We appreciate the valuable input of Patrick J. Hawkes for the analysis of the presented data.

Addendum

Subsequent to the acceptance of this paper, we have performed additional dosimetry measurements for the ''720 view, 4 frame per view'' and the ''360 view, 8 frames per view'' scan acquisition settings. The dosage for these scan settings are 38.9 REM (cGy) and 35.9 REM (cGy). We also determined the relative levels of noise for both acquisition settings on our instrument in a way that is applicable to other instruments: we measured the noise level by determining the standard deviation of CT value for a 1 × 1 × 1 cm volume of distilled, deionized water in a 50 ml plastic conical tube. For the ''720 view, 4 frame per view'' and the ''360 view, 8 frames per view'' scans the level of noise were 78 and 80.5 Hounsfield units, respectively.

References

[1] Carmeliet P, Jain RK (2000). Angiogenesis in cancer and other diseases. *Nature.* **407:**249–257.

[2] Duvall CL, Robert Taylor W, Weiss D, Guldberg RE (2004). Quantitative microcomputed tomography analysis of collateral vessel development after ischemic injury. *Am J Physiol Heart Circ Physiol.* **287:**H302–H310.

[3] Iwaki T, Yamashita H, Hayakawa T (2001). A color atlas of sectional anatomy of the mouse. Japan: Adthree Publishing Co., Ltd.

[4] Jain RK (2001). Normalizing tumor vasculature with anti-angiogenic therapy: A new paradigm for combination therapy. *Nat Med.* **7:**987–989.

[5] Keller C, Arenkiel BR, Coffin CM, El-Bardeesy N, DePinho RA, Capecchi MR (2004). Alveolar rhabdomyosarcomas in conditional Pax3:Fkhr mice: Cooperativity of Ink4a/ARF and Trp53 loss of function. *Genes Dev.* **18:**2614–2626.

[6] Kiessling F, Greschus S, Lichy MP, Bock M, Fink C, Vosseler S, Moll J, Mueller MM, Fusenig NE, Traupe H, Semmler W (2004). Volumetric computed tomography (VCT): A new technology for noninvasive, high-resolution monitoring of tumor angiogenesis. *Nat Med.* **10:**1133–1138.

[7] Kindlmann G, Durkin JW (1998). Semi-automatic generation of transfer functions for direct volume rendering. In *IEEE Symposium on Volume Visualization.* pp. 79–86.

[8] Levoy M (1988). Display of surfaces from volume data. *IEEE Comput Graph Appl.* **8:**29–37.

[9] Marxen M, Thornton MM, Chiarot CB, Klement G, Koprivnikar J, Sled JG, Henkelman RM (2004). MicroCT scanner performance and considerations for vascular specimen imaging. *Med Phys.* **31:**305–313.

[10] Möller T, Machiraju R, Mueller K, Yagel R (1997). Evaluation and design of filters using a Taylor series expansion. *IEEE Trans Vis Comput Graph.* **3:**184–199.

[11] Tufto I, Rofstad EK (1999). Interstitial fluid pressure and capillary diameter distribution in human melanoma xenografts. *Microvasc Res.* **58:**205–214.

[12] Weichert JP, Lee FT, Jr., Longino MA, Chosy SG, Counsell RE (1998). Lipid-based blood-pool CT imaging of the liver. *Acad Radiol.* **5:**S16–S19; discussion S28–S30.